C. R. Mecanique 338 (2010) 338–349

Contents lists available at ScienceDirect

Comptes Rendus Mecanique

www.sciencedirect.com

Steady state analysis of a hydrodynamic short bearing supplied with a circumferential groove

Sami Naïmi [a,*], Mnaouar Chouchane [a], Jean-Louis Ligier [b]

[a] Laboratoire génie mécanique, École nationale d'ingénieurs de Monastir, 5000 Tunisia
[b] RENAULT S.A., Powertrain Engineering Division, rue des Bons Raisins, 92508 Rueil Malmaison, France

ARTICLE INFO

Article history:
Received 27 February 2010
Accepted after revision 22 June 2010
Available online 10 July 2010

Keywords:
Lubrication
Short bearing theory
Hydrodynamic lubrication
Pressure profile
Circumferential feeding groove
Steady state analysis

ABSTRACT

A theoretical prediction of the steady state characteristics of a hydrodynamic short bearing with a circumferential central feeding groove is presented. An implicit relationship between the lubricant feeding pressure, the Sommerfeld number and the bearing eccentricity has been derived and used to investigate the effect of the feeding groove and supply pressure on the pressure field of the oil film and the bearing eccentricity. Curves relating the eccentricity to the Sommerfeld number for various supply pressures are presented and compared with published data obtained using numerical methods. A simplified explicit model has also been derived and shown to be useful for low Sommerfeld numbers. The steady state bearing characteristics predicted by the presented model are in good agreement with those of other published research work using other approaches.

1. Introduction

Hydrodynamic journal bearings are commonly used in various rotating machines with a range of design requirements. In a hydrodynamic regime, an oil film is formed between the journal and the bearing. Oil is usually supplied to the bearing through a hole or a groove in the low pressure region of the oil film; axial and circumferential feeding grooves may be used. A circumferential feeding groove is frequently used in applications where the applied load has a variable direction such as crankcase bearings and automotive turbocharger bearings. The pressure in the oil film in hydrodynamic lubrication is governed by a second order partial differential equation derived by Reynolds [1]. This equation was solved analytically by Sommerfeld [2] using the long bearing assumption and by Dubois and Ocvirk [3] in the case of a short bearing. The Sommerfeld assumption accounts for both positive and negative pressures in the lubricant film. This assumption is valid only if the applied load is low or the supply pressure is relatively high. Gümbel [4] neglected the negative pressures in the Sommerfeld solution leading to a discontinuity of the flow of the lubricant film. Although physically and mathematically unacceptable, this solution is frequently employed especially in the case of the short bearing theory since it allows for solutions in close agreement with experimental data [5,6]. More accurate solutions, particularly for finite length bearings, have been obtained using numerical methods to solve Reynolds equation by Christopherson [7] and Raimondi [8].

In the above cited references, it is usually assumed that the lubricant is supplied to the bearing through a hole or an axial groove located in the low pressure region of the oil film. For more accurate prediction of bearing characteristics, the effect of feeding solution has later been introduced in subsequent research work. Singh [9] considered the effect of the angular position of the axial supply groove on the static characteristics of the bearing. Roy [10] determined the static and dynamic

* Corresponding author.
E-mail address: sami.naimi@gmail.com (S. Naïmi).

1631-0721/$ – see front matter
doi:10.1016/j.crme.2010.06.003

Nomenclature

c	radial clearance
e, ε	eccentricity of journal bearing, eccentricity ratio $\varepsilon = e/c$
F, F_1, F_2	hydrodynamic film reaction for a conventional bearing, film reaction components
F_p, F_{1p}, F_{2p}	hydrodynamic film reaction for a bearing with circumferential groove, film reaction components
F_{sm}, F_{1sm}, F_{2sm}	hydrodynamic film reaction for the simplified model, film reaction components
$h, \bar{h}$	lubricant film thickness, dimensionless film thickness $\bar{h} = h/c$.
L, l	length of bearing (m), length of half bearing, $l = L/2$
$p, \bar{p}$	film pressure for a conventional bearing, dimensionless film pressure $\bar{p}(\theta, z) = 4p(\theta, z)c^2/(\mu\omega L^2)$
$p_p, \bar{p}_p$	film pressure for a bearing with circumferential groove, dimensionless film pressure $\bar{p}_p(\theta, z) = 4p_p(\theta, z)c^2/(\mu\omega L^2)$
$P_0, \bar{P}_0$	lubricant supply pressure, dimensionless lubricant supply pressure $\bar{P}_0 = 4P_0c^2/(\mu\omega L^2)$
$q, \bar{q}$	oil film force per unit length in the circumferential direction for a conventional bearing, dimensionless oil film force $\bar{q} = 4qc^2/(\mu\omega L^3)$
$q_p, \bar{q}_p$	oil film force per unit length in the circumferential direction for a bearing with circumferential groove, dimensionless oil film force $\bar{q}_p = 4q_pc^2/(\mu\omega L^3)$
R, D, r	radius of bearing, diameter of bearing and radius of journal
U	surface speed of journal
W_0	load applied on the journal
$z, \bar{z}$	axial coordinate, dimensionless axial coordinate $\bar{z} = 2z/L$
γ	attitude angle
θ	angular coordinate measured from the minimum film thickness position
μ	viscosity of film lubricant
σ	Sommerfeld number $\sigma = \mu L^3\omega R/(4c^2W_0)$
ω	angular velocity of journal
	Fig. 1 and Fig. 2 (a) and (b) illustrate the main geometrical parameters.

characteristics of a hydrodynamic bearing supplied with an axial groove using a numerical approach and investigated the effect of the angular position of the groove on static and dynamic characteristics of the bearing. Jeddi [11] applied the finite element method to solve Reynolds equation and studied the effect of the shape of the feeding groove and the supply pressure on the pressure profile. Crosby [12] presented an analytic analysis of cavitation in a short bearing supplied through a circumferential feeding groove. The oil film is divided into several zones and boundary conditions are specified for each zone so that an analytical solution to Reynolds equation is found for each zone. Jakeman [13] used the finite difference method to solve Reynolds equation including the effect of cavitation for crankshaft bearings supplied with circumferential central grooves.

In this paper, an analytical solution to Reynolds equation for a hydrodynamic short bearing lubricated under pressure through a circumferential central groove is presented. The groove divides the bearing into two narrow bearings. To solve Reynolds equation, appropriate boundary conditions are applied and negative pressures in the oil film are set to zero. Numerical integration of the pressure film is required to solve the explicit relationship between the eccentricity, the Sommerfeld number and the feeding pressure. The effect of the groove and the supply pressure on the pressure profile and the steady state characteristics of the bearing are investigated. A simplified analytical solution has also been derived applicable in a limited domain.

2. Theory

2.1. Reynolds equation

Hydrodynamic lubrication of a circular bearing by an incompressible and isoviscous fluid is governed by the following Reynolds equation [1]

$$\frac{1}{R^2}\frac{\partial}{\partial\theta}\left(\frac{h^3}{\mu}\frac{\partial p}{\partial\theta}\right) + \frac{\partial}{\partial z}\left(\frac{h^3}{\mu}\frac{\partial p}{\partial z}\right) = \frac{6U}{R}\frac{\partial h}{\partial\theta} + 12\frac{\partial h}{\partial t} \tag{1}$$

Reynolds equation is a second order partial differential equation for the pressure p; θ and z are respectively the circumferential and axial coordinates as shown in Fig. 1. Analytical solution to this equation is available if the bearing is assumed infinitely short or infinitely long. Numerical methods are usually applied to find the pressure distribution in the oil film for finite length bearings. This paper is concerned with hydrodynamic short bearings supplied with central circumferential groove as shown in Fig. 2. The groove divides the bearing into two narrow bearings; the length of each is usually small compared to its diameter. Using the short bearing assumption, the variation of pressure in the circumferential direction is neglected compared to that in the axial direction so that the first term in Eq. (1) is neglected compared to the second term. This assumption is usually justified for bearings with L/D ratios lower or equal to 1/8. In practice, this assumption

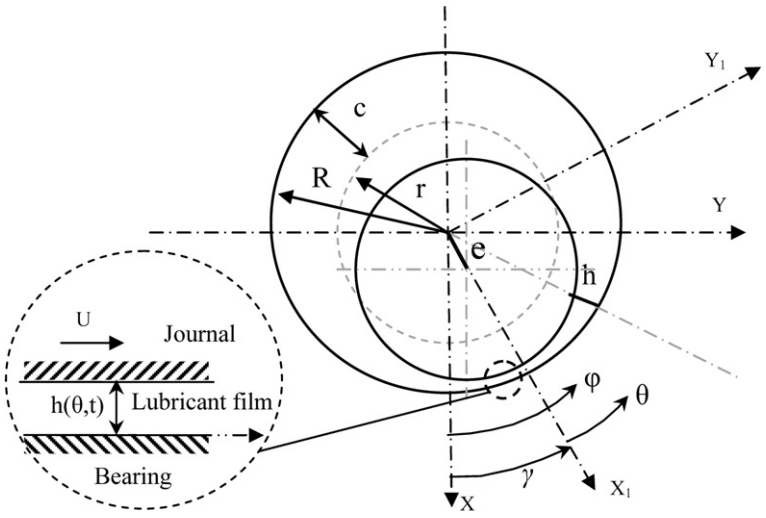

Fig. 1. Section of a hydrodynamic bearing.

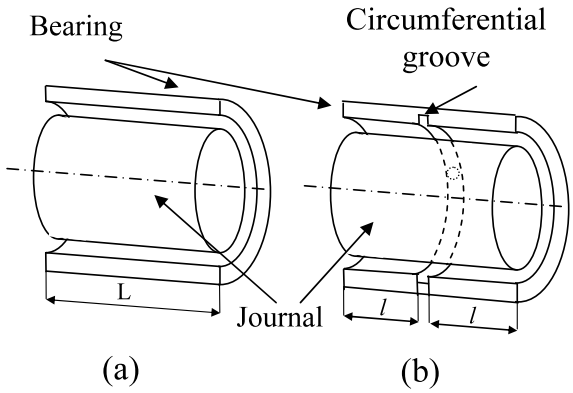

Fig. 2. Longitudinal section of a journal bearing: (a) conventional bearing; (b) bearing with circumferential feeding groove.

is sometime used for L/D ratios as high as $1/2$ because the error remains small on the torque and the flow. The error is usually acceptable for the load but is quite high on the maximum pressure in the oil film [5].

Thus, Eq. (1), under the short bearing assumption, can be reduced as follows

$$\frac{\partial}{\partial z}\left(\frac{h^3}{\mu}\frac{\partial p}{\partial z}\right) \simeq \frac{6U}{R}\frac{\partial h}{\partial \theta} + 12\frac{\partial h}{\partial t} \tag{2}$$

2.2. The pressure profile

The oil film thickness for a circular bearing at an angular position θ depends on the radial clearance c and the eccentricity ratio $\varepsilon = \frac{e}{c}$, Fig. 1, and does not depend on the axial position z if the effect of misalignment is neglected. Thus,

$$h(\theta, t) = c\big(1 - \varepsilon(t)\cos\theta\big) \tag{3}$$

Substituting the time derivative of oil film thickness h in Eq. (2) and assuming a constant viscosity μ, the following equation is obtained

$$\frac{\partial^2 p}{\partial z^2} = \frac{6\mu c}{h^3(\theta, t)}\big(\varepsilon(\omega - 2\dot{\gamma})\sin\theta - 2\dot{\varepsilon}\cos\theta\big) \tag{4}$$

where γ is the attitude angle and ω the angular velocity of journal.

A double integration of the above equation with respect to z gives

$$p(\theta, z, t) = \frac{3\mu c}{h^3(\theta, t)}\big(\varepsilon(\omega - 2\dot{\gamma})\sin\theta - 2\dot{\varepsilon}\cos\theta\big)z^2 + C_1 z + C_2 \tag{5}$$

where C_1 and C_2 are two integration constants determined by applying the boundary conditions.

In a steady state condition, $\dot{\gamma} = \dot{\varepsilon} = 0$, so that Eq. (5) reduces to

$$p(\theta, z) = \frac{3\mu c}{h^3}(\varepsilon\omega \sin\theta)z^2 + C_1 z + C_2 \tag{6}$$

In the conventional short bearing theory, it is assumed that the bearing is supplied through a hole or an axial groove located in the low pressure zone of the oil film and the ends of the bearing are subjected to the atmospheric pressure. Thus, if the origin of the z axis is chosen at the middle of the bearing, the following boundary conditions are applied

$$p(\theta, z = \pm L/2) = 0; \quad \forall\theta$$

Consequently, the following pressure profile is obtained

$$p(\theta, \bar{z}) = \frac{\mu\omega L^2}{4c^2}\bar{p}(\theta, \bar{z}) \tag{7}$$

where

$$\bar{p}(\theta, \bar{z}) = \frac{3\varepsilon \sin\theta}{(1 - \varepsilon\cos\theta)^3}\left(\bar{z}^2 - 1\right) \tag{8}$$

and

$$\bar{z} = \frac{2z}{L}$$

A short hydrodynamic bearing of length L, having a central circumferential feeding groove, forms two infinitely short half bearings having each a length $l = L/2$.

Considering now one half bearing and choosing the origin of the z axis at the middle of the half bearing, the lubricant is supplied through the groove at a constant supply pressure P_0, the boundary conditions for the half bearing are

$$p(\theta, z = l/2) = P_0; \quad p(\theta, z = -l/2) = 0; \quad \forall\theta$$

Using Eq. (6) and applying the above boundary conditions, the following pressure p_p in a one half bearing is obtained

$$p_p(\theta, z) = \frac{\mu\omega L^2}{4c^2}\bar{p}_p(\theta, \bar{z}) \tag{9}$$

where

$$\bar{p}_p(\theta, \bar{z}) = \frac{3\varepsilon \sin\theta}{(1 - \varepsilon\cos\theta)^3}\left(\bar{z}^2 - \frac{1}{4}\right) + \bar{P}_0\left(\bar{z} + \frac{1}{2}\right)$$
$$\bar{z} = \frac{2z}{L} \quad \text{and} \quad \bar{P}_0 = \frac{4c^2}{\mu\omega L^2}P_0 \tag{10}$$

Both dimensionless pressure profiles, defined by Eqs. (8) and (10), contain regions with negative pressures. To determine the hydrodynamic reactions using Sommerfeld boundary conditions [2], the pressure profile including negative pressures is used. In another more admitted approach, proposed by Gûmbel, negative pressure region is considered to be a cavitation zone and thus negative pressures are set to zero. For a conventional bearing, the negative pressure zone covers roughly half of the film. The following pressure profile is therefore used

$$p(\theta, \bar{z}) = 0, \quad \theta \in [0,\ \pi] \tag{11}$$

For a bearing with a central circumferential groove, the positive pressures may cover more than half of the oil film. Thus, the pressure is computed for the whole film using Eq. (10) and then negative pressure are set to zero. So that

$$p_p(\theta, \bar{z}) = 0, \quad \text{if } p_p(\theta, \bar{z}) \leqslant 0 \tag{12}$$

2.3. Circumferential distribution of the hydrodynamic reaction

For a conventional bearing, the oil film reaction par unit length in the circumferential direction $q(\theta)$ is found by integrating with respect to z the pressure distribution $p(\theta, \bar{z})$ defined by Eq. (11)

$$q(\theta) = \int_{-1}^{1} p(\theta, \bar{z}) L\, \mathrm{d}\bar{z} = \frac{\mu L^3 \omega}{4c^2}\bar{q}(\theta) \tag{13}$$

where

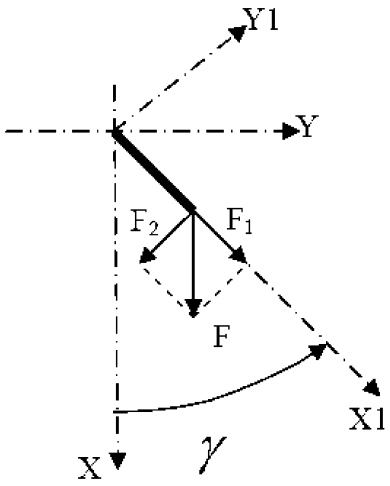

Fig. 3. Hydrodynamic oil reaction components.

$$\begin{cases} \bar{q}(\theta) = \dfrac{1}{2}\dfrac{\varepsilon \sin\theta}{(1-\varepsilon\cos\theta)^3}, & \theta \in [\pi,\ 2\pi] \\ \text{and } \bar{q}(\theta) = 0, & \theta \in [0,\ \pi] \end{cases}$$

For a bearing with oil supply through a circumferential central groove, the oil film reaction par unit length in the circumferential direction $q_p(\theta)$ is found by numerical integration of the pressure $p_p(\theta, \bar{z})$ in the active zone.

$$q_p(\theta) = 2\int_{-1/2}^{1/2} p_p(\theta,\bar{z})\frac{L}{2}\,\mathrm{d}\bar{z} = \frac{\mu\omega L^3}{4c^2}\bar{q}_p(\theta) \tag{14}$$

where

$$\bar{q}_p(\theta) = \int_{-1/2}^{1/2} \bar{p}_p(\theta,\bar{z})\,\mathrm{d}\bar{z}$$

The above equation accounts for the two half bearings.

2.4. Hydrodynamic oil film reactions

For a conventional bearing, the hydrodynamic force components F_1 and F_2 along respectively the axis (X_1, Y_1), shown in Fig. 3, are found by integration of the circumferential force distribution $q(\theta)$ along the circumference of the bearing.

$$\begin{aligned} F_1 &= \int_0^{2\pi} q(\theta)\cos\theta R\,\mathrm{d}\theta = \frac{\mu R L^3\omega}{2c^2}\int_\pi^{2\pi} \bar{q}(\theta)\cos\theta\,\mathrm{d}\theta = F_0 f_1(\varepsilon) \\ F_2 &= \int_0^{2\pi} q(\theta)\sin\theta R\,\mathrm{d}\theta = \frac{\mu R L^3\omega}{2c^2}\int_\pi^{2\pi} \bar{q}(\theta)\sin\theta\,\mathrm{d}\theta = F_0 f_2(\varepsilon) \end{aligned} \tag{15}$$

where

$$F_0 = \frac{\mu R L^3\omega}{2c^2} \tag{16}$$

and

$$\begin{aligned} f_1(\varepsilon) &= \frac{2\varepsilon^2}{(1-\varepsilon^2)^2} \\ f_2(\varepsilon) &= -\frac{\pi}{2}\frac{\varepsilon}{(1-\varepsilon^2)^{3/2}} \end{aligned} \tag{17}$$

The resulting hydrodynamic force F is thus,

$$F = \sqrt{F_1^2 + F_2^2} \tag{18}$$

For a bearing supplied with a circumferential central groove, the hydrodynamic force components F_{p1} and F_{p2} are computed by numerical integration of the circumferential force distribution in the oil film region with positive pressures

$$F_{p1} = \int_0^{2\pi} q_p(\theta)\cos\theta R\,\mathrm{d}\theta = \frac{\mu R L^3 \omega}{2c^2}\int_0^{2\pi} \bar{q}_p(\theta)\cos\theta\,\mathrm{d}\theta = F_0 f_{p1}(\varepsilon, \bar{P}_0)$$
$$F_{p2} = \int_0^{2\pi} q_p(\theta)\sin\theta R\,\mathrm{d}\theta = \frac{\mu R L^3 \omega}{2c^2}\int_0^{2\pi} \bar{q}_p(\theta)\sin\theta\,\mathrm{d}\theta = F_0 f_{p2}(\varepsilon, \bar{P}_0) \tag{19}$$

It should be noted that in the above equation, $\bar{q}_p(\theta)$ is defined by Eq. (14) and F_0 is defined by Eq. (16). To compute the dimensionless forces f_{p1} and f_{p2}, the eccentricity ε and the dimensionless pressure $\bar{P}_0$ have to be specified. The pressure distribution is computed first by Eq. (10) then a numerical integration is required to find the circumferential force distribution $\bar{q}_p(\theta)$ using Eq. (14). Finally, a second numerical integration of Eq. (14) is needed to compute the dimensionless forces f_{p1} and f_{p2}. The resulting hydrodynamic oil film reaction can, then, be found

$$F_p = \sqrt{F_{p1}^2 + F_{p2}^2} \tag{20}$$

2.5. Eccentricity ratio and attitude angle

For a conventional hydrodynamic bearing at steady state equilibrium, the load W_0 applied on the journal is balanced by the hydrodynamic force F applied by the oil film

$$W_0 = F = \frac{\mu\omega R L^3}{c^2}\frac{\varepsilon}{4}\frac{\sqrt{16\varepsilon^2 + \pi^2(1-\varepsilon^2)}}{(1-\varepsilon^2)^2} \tag{21}$$

For a short bearing, the Sommerfeld number is usually defined as

$$\sigma = \frac{\mu L^3 \omega R}{4c^2 W_0} \tag{22}$$

Substituting W_0 from Eq. (21) in Eq. (22), the following relation between the Sommerfeld number and the eccentricity ratio is found

$$\sigma = \frac{(1-\varepsilon^2)^2}{\varepsilon\sqrt{16\varepsilon^2 + \pi^2(1-\varepsilon^2)}} \tag{23}$$

The attitude angle γ defined in Fig. 3 is computed using the oil film force components F_1 and F_2

$$\tan\gamma = -\frac{F_2}{F_1} = \frac{\pi\sqrt{(1-\varepsilon^2)}}{4\varepsilon} \tag{24}$$

For a bearing with a central circumferential groove in steady state equilibrium, the external load W_0 applied on the journal, is balanced by the hydrodynamic force F_p applied by the oil films of the two half bearings

$$F_p = F_0\sqrt{f_{p1}(\varepsilon, \bar{P}_0)^2 + f_{p2}(\varepsilon, \bar{P}_0)^2} = W_0 \tag{25}$$

In this case, the relationship between the Sommerfeld number and the eccentricity ratio is written as

$$\sigma = \frac{1}{\sqrt{f_{p1}(\varepsilon, \bar{P}_0)^2 + f_{p2}(\varepsilon, \bar{P}_0)^2}} \tag{26}$$

For a given eccentricity ratio ε and a dimensionless pressure $\bar{P}_0$, Eq. (26) along with Eqs. (14) and (19) are used to compute the Sommerfeld number σ. In a more practical case, the Sommerfeld number σ and dimensionless pressure $\bar{P}_0$ are specified and therefore the eccentricity ratio ε is computed using an iterative procedure.

The attitude angle γ is computed using the following equation

$$\tan\gamma = -\frac{F_{p2}}{F_{p1}} = -\frac{f_{p2}(\varepsilon, \bar{P}_0)}{f_{p1}(\varepsilon, \bar{P}_0)} \tag{27}$$

2.6. Simplified steady state solution

The drawback of the computation method presented in Sections 2.3, 2.4 and 2.5 is that two numerical integrations are required successively in Eqs. (14) and (19) to compute the hydrodynamic film reactions. Thus, an implicit relation exists between the eccentricity ratio ε, the Sommerfeld number σ and the dimensionless pressure $\bar{P}_0$. In this section, a simplified solution is presented in which no numerical integration is required and therefore a direct and explicit relation is established between the eccentricity ratio ε, the Sommerfeld number σ and the feeding pressure $\bar{P}_0$. To avoid numerical integration, the oil film pressures are set to zero for circumferential angles $\theta \in [0, \pi]$ in a way similar to the half Sommerfeld assumption of π film and the integration in Eq. (19) is limited to the domain $\theta \in [\pi, 2\pi]$. The impact of the proposed simplification shall be investigated in Section 3. Film reaction components F_{1s} and F_{2s} can now be obtained by analytical integration of the circumferential force distribution

$$F_{1sm} = LR \int_{-1/2}^{1/2} \int_{\pi}^{2\pi} p(\theta, \bar{z}) \cos\theta \, \mathrm{d}\theta \, \mathrm{d}\bar{z} = \frac{\mu L^3 \omega R}{8c^2} f_1(\varepsilon)$$

$$F_{2sm} = LR \int_{-1/2}^{1/2} \int_{\pi}^{2\pi} p(\theta, \bar{z}) \sin\theta \, \mathrm{d}\theta \, \mathrm{d}\bar{z} = \frac{\mu L^3 \omega R}{8c^2} f_2(\varepsilon) - P_0 RL \tag{28}$$

The dimensionless force components $f_1(\varepsilon)$ and $f_2(\varepsilon)$ are given in Eq. (17).

The equilibrium between the load W_0 applied on the journal and the hydrodynamic force F_{sm} applied by both oil films of the half bearings can be written as

$$F_{sm} = \frac{\mu L^3 \omega R}{8c^2} \sqrt{\frac{4\varepsilon^4}{(1-\varepsilon^2)^4} + \left(\frac{\pi}{2} \frac{\varepsilon}{(1-\varepsilon^2)^{3/2}} + \frac{8 P_0 c^2}{\mu \omega L^2} \right)^2} = W_0 \tag{29}$$

Eqs. (22) and (29) can be written in the form of a relationship between the Sommerfeld number σ, the eccentricity ratio ε and the dimensionless supply pressure $\bar{P}_0$.

$$\sigma = \frac{1}{\sqrt{\frac{\varepsilon^4}{(1-\varepsilon^2)^4} + \left(\frac{\pi}{4} \frac{\varepsilon}{(1-\varepsilon^2)^{3/2}} + \bar{P}_0 \right)^2}} \tag{30}$$

The attitude angle is determined using the oil film components F_{1sm} and F_{2sm} given in Eq. (28)

$$\tan\gamma = -\frac{F_{2sm}}{F_{1sm}} = \frac{\pi\sqrt{(1-\varepsilon^2)}}{4\varepsilon} + \frac{\bar{P}_0 (1-\varepsilon^2)^2}{\varepsilon^2} \tag{31}$$

Eqs. (30) and (31) establish an explicit relation between the eccentricity ratio ε, the Sommerfeld number σ, the dimensionless pressure $\bar{P}_0$ and the attitude angle γ contrary to Eqs. (26) and (27) which establish a rather implicit relation between these four quantities.

3. Results and discussion

Applying the short bearing theory, the 3D pressure profiles and the iso-value pressure curves for a conventional bearing with low and high eccentricity ratios, $\varepsilon = 1/4$ and $\varepsilon = 3/4$, are shown, respectively, in Figs. 4 and 5. The negative pressures are set to zero in these figures. The pressure profiles are symmetrical with respect to the bearing median axis. The maximum dimensionless pressure for $\varepsilon = 1/4$ and $\varepsilon = 3/4$ are respectively, 0.97 and 29.91 at circumferential angles, 306° and 339°. The pressure profiles of Figs. 4 and 5 are computed using Eq. (8). It should be noted that positive pressures are confined to half of the film, for both eccentricities. For the other half of the oil film, the film may not be completely formed. The maximum pressure is significantly higher for $\varepsilon = 3/4$ than for $\varepsilon = 1/4$ and located at an angle closer to the angle of minimum film thickness. Figs. 6 and 7 show the pressure profiles for the same eccentricities ε as those of Figs. 4 and 5 in the case where lubricant is supplied to the bearing through a central circumferential groove at a dimensionless pressure $\bar{P}_0 = 0.24$. Eq. (10) has been used to compute the pressure profiles of Figs. 6 and 7. The selected particular dimensionless feeding pressure, $\bar{P}_0 = 0.24$, is identical to that of Ref. [13] which will be used for the validation of the proposed solution at the end of this section. The pressure profiles are symmetrical with respect to the circumferential feeding groove. The maximum dimensionless pressures for $\varepsilon = 1/4$ and $\varepsilon = 3/4$ are respectively, 0.37 and 7.59 at circumferential angles 306° and 339°. For the considered feeding pressure, the maximum dimensionless pressures are lower than those of a conventional bearing for $\varepsilon = 1/4$ and $\varepsilon = 3/4$. The maximum pressure is reduced by a factor of 61% for $\varepsilon = 1/4$ and 74% for $\varepsilon = 3/4$. The axial position of the maximum pressure is not centred for each half bearing but slightly shifted towards the side of the supply groove but the circumferential position of the maximum pressure is the same for a conventional bearing and a bearing with circumferential groove. The positive pressure region expands for an area larger than half of the oil film. The positive pressure area is larger for $\varepsilon = 1/4$ than for $\varepsilon = 3/4$.

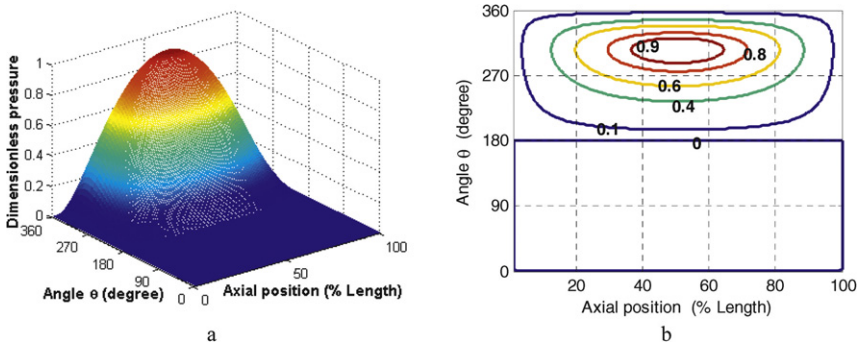

Fig. 4. Dimensionless pressure profile for $\varepsilon = 1/4$: (a) 3D profile; (b) iso-values curves.

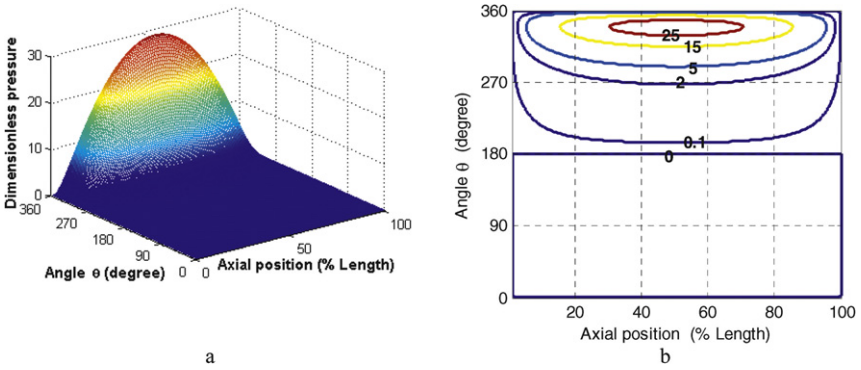

Fig. 5. Dimensionless pressure profile for $\varepsilon = 3/4$: (a) 3D profile; (b) iso-values curves.

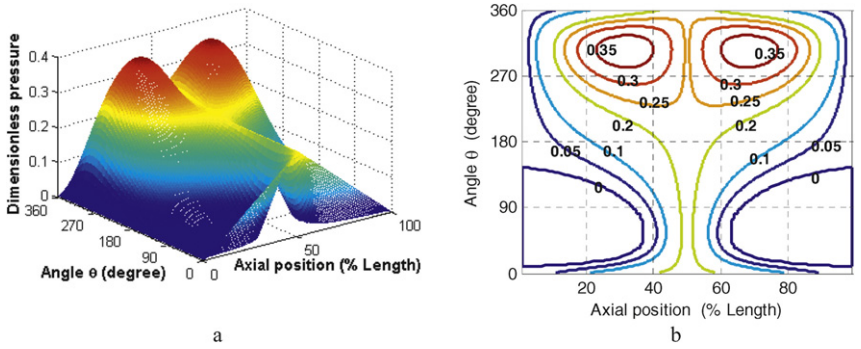

Fig. 6. Dimensionless pressure profile: $\varepsilon = 1/4$ and $\bar{P}_0 = 0.24$: (a) 3D profile; (b) iso-values curves.

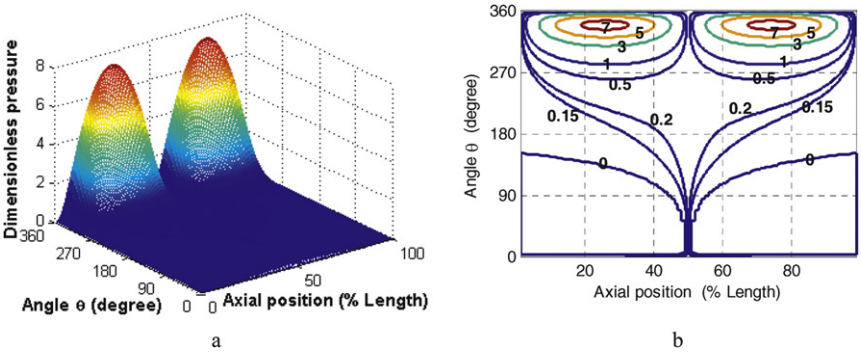

Fig. 7. Dimensionless pressure profile: $\varepsilon = 3/4$ and $\bar{P}_0 = 0.24$: (a) 3D profile; (b) iso-values curves.

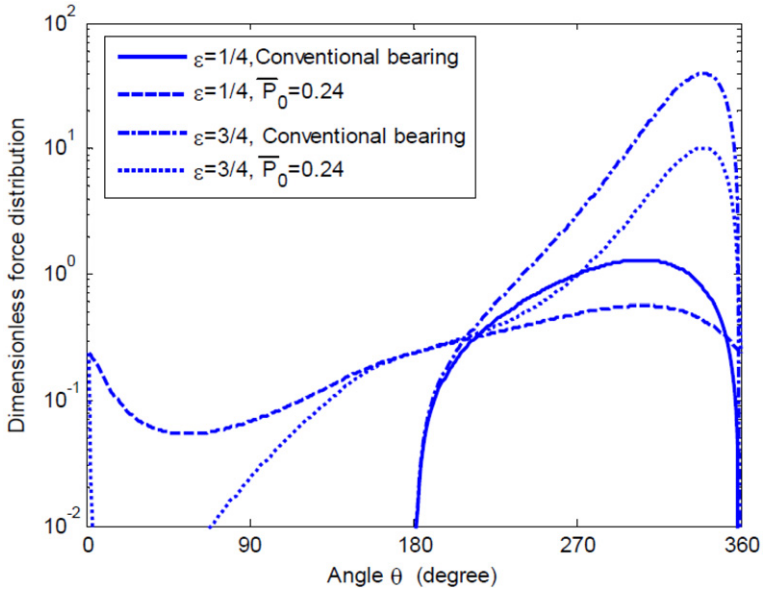

Fig. 8. Dimensionless circumferential force distribution $\bar{q}(\theta)$ for two dimensionless supply pressures $\bar{P}_0$ and two eccentricity ratios ε.

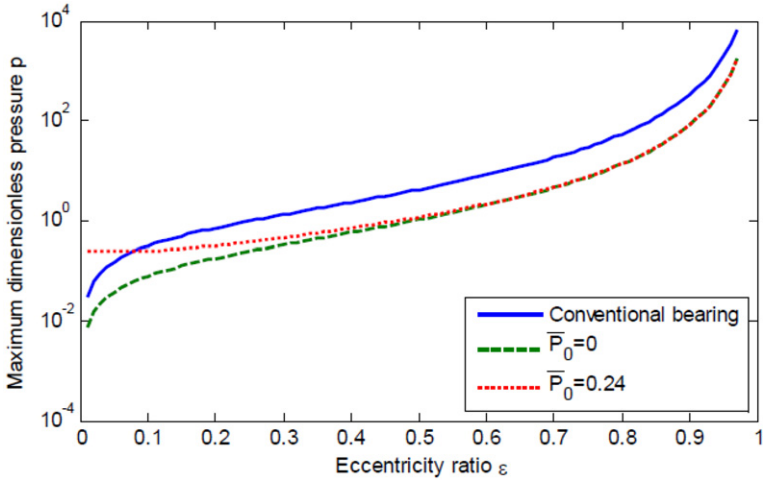

Fig. 9. The maximum dimensionless pressure for a conventional bearing and for two supply pressures.

Fig. 8 shows the force per unit length distribution in the circumferential direction for the eccentricities $\varepsilon = 1/4$ and $\varepsilon = 3/4$ for both cases: a conventional bearing and a bearing with feeding groove. Hydrodynamic forces are confined to half of the circumference of the bearing for the former and cover a larger angle for the latter particularly for an eccentricity $\varepsilon = 1/4$. The variation of maximum pressure with eccentricity ε is depicted in Fig. 9 for a conventional bearing and for a feeding under atmospheric pressure, $\bar{P}_0 = 0$, and a dimensionless pressure $\bar{P}_0 = 0.24$. The maximum pressure in the oil film increases with eccentricity for the considered supply pressures and is higher for a conventional bearing except for very small eccentricities and relatively high supply pressure. The circumferential angular position of the maximum oil film pressure increases with the eccentricity ratio, as shown in Fig. 10, and is the same for either conventional bearing or a bearing supplied with a circumferential groove. The increase of supply pressure seems to have no effect on the maximum pressure angular position.

Similarly to a conventional bearing, the eccentricity ratio ε of a bearing with a central circumferential groove decreases with Sommerfeld number σ, Fig. 11. However, for a given Sommerfeld number, the eccentricity is higher for the latter.

The attitude angle increases with Sommerfeld number as shown in Fig. 12. Compared to a conventional bearing, the attitude angle is lower at low Sommerfeld numbers and is higher for high Sommerfeld numbers for high feeding pressures.

The relative eccentricity ε and attitude angle γ predicted using the simplified solutions of Eqs. (30) and (31) versus Sommerfeld number are shown respectively in Figs. 13 and 14 and compared with the curves of Figs. 11 and 12. The simplified model agrees with the full model for low Sommerfeld numbers and low supply pressures.

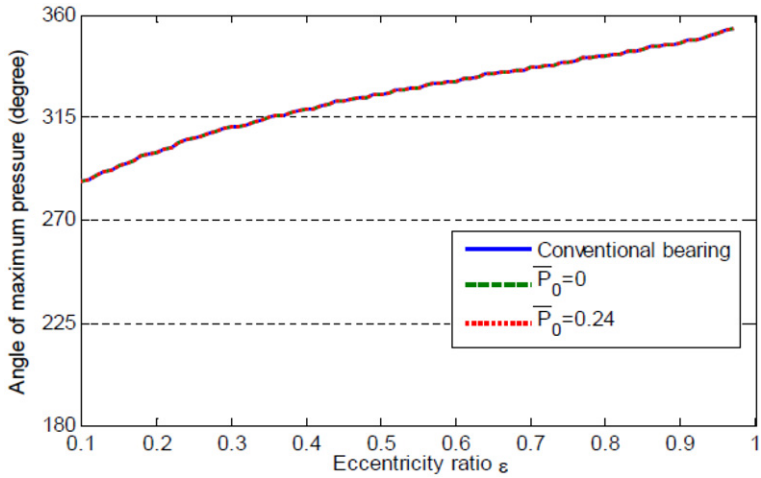

Fig. 10. Variation of the angular position of the maximum pressure with eccentricity ratio. (The three curves are identical.)

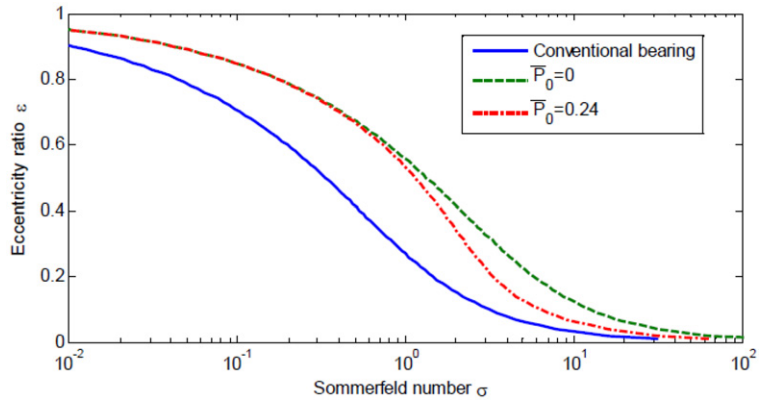

Fig. 11. Variation of the eccentricity ratio with Sommerfeld number.

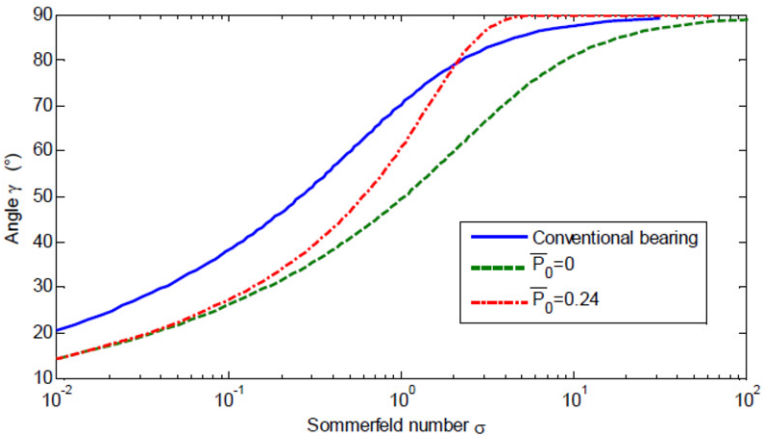

Fig. 12. Variation of the attitude angle with Sommerfeld number.

To assess the quality of prediction of the full and simplified models introduced in this paper, a comparison is attempted with the results published by Crosby [12]. The results of this reference are obtained by an analytical solution of the pressure field in which the cavitation in the oil film is accounted for. Fig. 15 shows that the variation of the eccentricity with Sommerfeld number obtained in [12] is in good agreement with the full model proposed in this paper for the two supply pressures $\bar{P}_0 = 0$ and $\bar{P}_0 = 0.24$. Results from the simplified model also agree with those of Crosby for a feeding under atmospheric pressure but correlate with those of Crosby only at low Sommerfeld number for a feeding pressure $\bar{P}_0 = 0.24$.

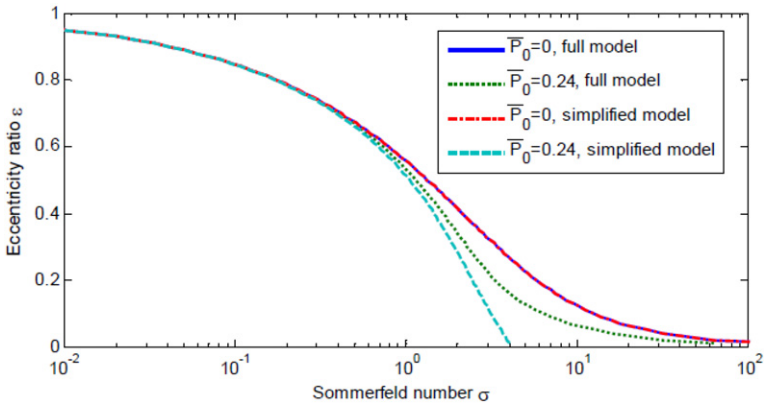

Fig. 13. Sommerfeld number and eccentricity ratio for the full and simplified model.

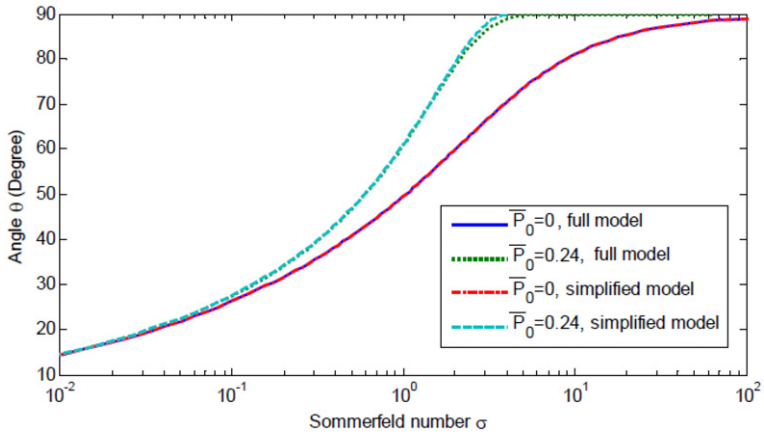

Fig. 14. Attitude angle versus Sommerfeld number for the full and simplified model.

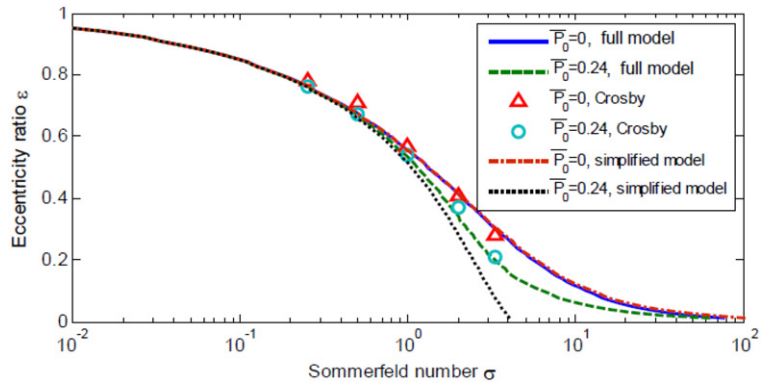

Fig. 15. Eccentricity in different model.

In Table 1, the predicted static load W_0 and the attitude angle γ by the full and the simplified models are compared with those of Parkins [14] and Jakeman [13] for a set of bearing data obtained numerically using the finite difference method and Jakeman has applied a cavitation model.

The results from the full model present a variation which does not exceed 18% for the attitude angle and 26% for the hydrodynamic force compared to those of Jakeman and Parkins. The simplified model results are close to those found by the full model because only high eccentricity ratios are considered, 0.79 to 0.942 and both models agree for low Sommerfeld numbers and high eccentricity ratios as shown in Fig. 13.

Table 1
Static load and attitude angle obtained by different approaches.

Commun input data				Full model		Simplified model		Parkins [14]		Jakeman [13]	
ε	μ (Pa.s)	ω (rpm)	c (mm)	W_0 (N)	γ^o	W_0 (N)	γ^o	W_0 (N)	γ^o	W_0 (N)	γ^o
0.790	0.04470	1180	0.04545	707.5	38.48	650.9	39.07	670.2	38.70	683.2	39.28
0.864	0.04139	1180	0.04705	1493.2	27.90	1461.0	28.65	1341.2	30.60	1352.0	31.59
0.869	0.01883	2200	0.04500	1494.8	27.37	1465.2	28.20	1285.2	31.84	1323.9	33.16
0.902	0.02897	1500	0.04760	2541.1	22.49	2523.9	23.11	2219.2	24.00	2212.0	24.84
0.917	0.01069	2900	0.04680	2621.3	20.56	2613.3	21.31	2230.3	23.30	2182.2	24.49
0.926	0.02414	1500	0.04840	3626.7	19.00	3621.3	19.56	3120.3	19.60	3044.6	20.29
0.930	0.01552	2200	0.04915	3714.7	18.43	3711.8	19.00	3125.0	18.70	3091.5	19.15
0.942	0.008794	2900	0.05015	3886.2	16.67	3891	17.33	3113.2	18.00	3089.6	18.63
$L/D = 0.29$; $P_0 = 0.2067$ N/mm^2											

4. Conclusion

The effect of a central circumferential feeding groove on the steady state characteristics of a hydrodynamic short bearing is investigated. The results are summarized as follows:

(i) A circumferential central groove divides the bearing into two half bearings and decreases the maximum oil film pressure for a given eccentricity.
(ii) A higher supply pressure increases the oil film maximum pressure in each half bearing, expands the region of positive pressures, shifts the maximum pressure position towards the feeding groove side and leaves invariant its circumferential angular position.
(iii) The feeding through a circumferential groove affects steady state equilibrium, for a given Sommerfeld number. The presence of the groove increases the eccentricity ratio and decreases the attitude angle compared to a conventional bearing. The increase of supply pressure decreases the eccentricity and increases the attitude angle.

A simplified model for the prediction of the steady state equilibrium has also been derived. It is simple to use and establishes an explicit relation between the Sommerfeld number, the feeding dimensionless pressure and the eccentricity ratio. However, this model is not accurate for high Sommerfeld numbers.

Acknowledgements

This research is funded and supported by:

- Ministry of Higher Education and Scientific Research, Tunisia.
- RENAULT S.A.S. (Powertrain Engineering Division), French.

References

[1] O. Reynolds, On the theory of lubrication and its application to Mr. Beauchamps Tower's Experiments, including an experimental determination of the viscosity of olive oil, Phil. Trans. Roy. Soc. (London) A 177 (1889) 157–234.
[2] A. Sommerfeld, Zur Hydrodynamischen Theorie der Schmiermittel-Reibung, Zeitschrift für Math. Physik 40 (1904) 97–155.
[3] G.B. Dubois, F.W. Ocvirk, Analytical derivation and experimental evaluation of short bearing approximations of full journal bearings, NACA 1953, Tech. rep. 1157.
[4] L. Gümbel, Verleich der Ergebnisse der rechnerischen Behandlung des Lagerschmierungsproblem mit neueren Versuchsergebnissen, Monatsblätter Berlin.Bez.- V.D.I. (Sep. 1921) 125–128.
[5] J. Frêne, D. Nicolas, B. Deugueurce, D. Bertae, M. Godet, Hydrodynamic Lubrication: Bearing and Thrust Bearings, Tribology Series, vol. 33, Elsevier, 1997.
[6] Y. Hori, Hydrodynamic Lubrication, Springer-Verlag, Tokyo, 2006.
[7] D.G. Christopherson, A new mathematical method for the solution of film lubrication problems, Proc. Inst. Mech. Eng. 35 (00) (1941), 146:126.
[8] A.A. Raimondi, J.A. Boyd, A solution for the finite journal bearing and its application to analysis and design, I, II and III, ASLE Trans. 1 (1958) 159–209.
[9] U. Singh, L. Roy, M. Sahu, Steady state thermo-hydrodynamic analysis of cylindrical fluid film journal bearing with axial groove, Tribology International 41 (2008) 1135–1144.
[10] L. Roy, S.K. Laha, Steady state and dynamic characteristics of axial grooved journal bearings, Tribology International 42 (2008) 754–761.
[11] L. Jeddi, M. El Khlifi, D. Bonneau, Effets de la forme de la rainure d'alimentation d'un palier sur l'écoulement hydrodynamique, le débit et la distribution de la pression, Mécanique & Industries 5 (2004) 685–691.
[12] W.A. Crosby, Analytical prediction of cavity interface and bearing performance in a short bearing with circumferential feeding, Wear 136 (1990) 237–253.
[13] R.W. Jakeman, A numerical analysis method based on flow continuity for hydrodynamic journal bearings, Tribology International 17 (6) (1984).
[14] D.W. Parkins, Static and dynamic characteristics of an hydrodynamic journal bearing, PhD thesis, Cranfield Inst. Technol., May 1976.